
Iodine Symporter Targeting with $^{124}\text{I}/^{131}\text{I}$ Theranostics

James Nagarajah^{1,2}, Marcel Janssen¹, Philipp Hetkamp², and Walter Jentzen²

¹Department of Radiology and Nuclear Medicine, Radboud University Nijmegen Medical Centre, Nijmegen, The Netherlands; and

²Department of Nuclear Medicine, University of Duisburg–Essen, Duisburg, Germany

Theranostics, a modern approach combining therapeutics and diagnostics, is among the most promising concepts in nuclear medicine for optimizing and individualizing treatments for many cancer entities. Theranostics has been used in clinical routines in nuclear medicine for more than 60 y—as ^{131}I for diagnostic and therapeutic purposes in thyroid diseases. In this minireview, we provide a survey of the use of 2 different radioiodine isotopes for targeting the sodium–iodine symporter in thyroid cancer and non-thyroidal neoplasms as well as a brief summary of theranostics for neuroendocrine neoplasms and metastatic castration-refractory prostate cancer. In particular, we discuss the role of ^{124}I -based dosimetry in targeting of the sodium–iodine symporter and describe the clinical application of ^{124}I dosimetry in a patient who had radioiodine-refractory thyroid cancer and who underwent a redifferentiation treatment with the mitogen-activated extracellular signal–related kinase inhibitor trametinib.

Key Words: iodine theranostics; sodium–iodine symporter; redifferentiation; trametinib; breast cancer

J Nucl Med 2017; 58:34S–38S

DOI: 10.2967/jnumed.116.186866

Theranostics is a diagnostic approach coupled with treatment modalities in a personalized fashion to improve therapeutic effects and reduce treatment toxicities (1). This term was initially coined by John Funkhouser in a 1998 press release in connection with personalized treatment. Translating theranostics to the field of nuclear medicine means labeling of a compound with different radionuclides for both diagnostic and therapeutic purposes for a specific target. Ideally, the radionuclides used for both diagnostic and therapeutic purposes are derived from the same element, but for chemical and physical reasons this is often not practicable. In this mini review, we provide a brief survey of 2 theranostic approaches for neuroendocrine tumors and prostate cancer, with a focus on targeting of the sodium–iodine symporter (NIS) in thyroidal disorders, and we discuss issues regarding ^{124}I and ^{131}I targeting of the NIS in extrathyroidal disorders.

CLINICAL USE OF THERANOSTIC AGENTS OTHER THAN IODINE

Neuroendocrine neoplasms and prostate cancer are currently the most prominent targets of nonthyroidal theranostic agents (2–4). Because of a lack of efficient treatment options, metastatic, well-differentiated neuroendocrine neoplasms are challenging tumors. These tumors express somatostatin receptors, which can be imaged by PET with, for instance, ^{68}Ga -labeled DOTATATE, DOTATOC, or DOTANOC (5). PET enables in vivo quantification of the tumoral expression level and of the background uptake level in the surrounding tissues or organs at risk. For treatment, the same compound can be labeled with a β -particle emitter (^{177}Lu or ^{90}Y) to target metastatic sites. The higher the level of expression in the tumor (and, thus, the higher the tumor-to-background ratio), the lower the radiation-related toxicity effects in the surrounding tissues.

Regarding toxicity, protection of the kidneys is important, because a large portion of the injected amount of a radiolabeled compound is eliminated via renal excretion. To address this issue, patients receive an infusion of an amino acid cocktail during treatment to saturate renal reabsorption mechanisms (6). The efficacy of this approach was recently shown in a prospective multicenter trial (2).

Another promising theranostic approach is being used for metastatic castration-resistant prostate cancer. The target in this challenging disease is the prostate-specific membrane antigen (PSMA), which is expressed at high levels, particularly in recurrent prostate cancer; additionally, expression is not lost with dedifferentiation, making it an ideal target. PSMA-targeting molecules can be labeled with different positron emitters, such as ^{124}I , ^{18}F , ^{64}Cu , or ^{68}Ga (3,7). At present, PSMA ligands are more frequently labeled with ^{68}Ga for PET imaging. For therapeutic purposes, they are usually labeled with the β -particle emitter ^{177}Lu . However, there has even been a report on the labeling of a PSMA ligand with the α -particle emitter ^{225}Ac for the treatment of patients whose disease progressed after ^{177}Lu -PSMA ligand treatment (8).

THERANOSTICS WITH IODINE

Radioiodine treatment (using ^{131}I) has been the main pillar of nuclear medicine for more than 60 y. ^{131}I not only is a β -particle emitter but also has penetrating γ -radiation, which makes this tracer trackable in vivo through imaging. However, ^{131}I is not the ideal tracer for quantitative imaging purposes because of poor spatial resolution and quantification capacity using SPECT (Table 1). With the increasing availability of PET scanners during the last 15 y, ^{124}I became the tracer of first choice for the imaging of thyroid disorders, mainly in patients with high-risk and recurrent thyroid cancer (9,10). The properties of ^{124}I and ^{131}I are juxtaposed in Table 1, demonstrating the superiority of ^{124}I for imaging. Moreover, ^{124}I allows more reliable dosimetry, the 2 main pillars of which are shown in Figure 1.

Received Mar. 16, 2017; revision accepted May 31, 2017.

For correspondence or reprints contact: James Nagarajah, Department of Radiology and Nuclear Medicine, Radboud University Nijmegen Medical Centre, P.O. Box 9101, 6500 HB Nijmegen, The Netherlands.

E-mail: james.nagarajah@radboudumc.nl

COPYRIGHT © 2017 by the Society of Nuclear Medicine and Molecular Imaging.

TABLE 1

Physical Half-Lives and Qualitative Comparison of Common Radioiodine Isotopes for Imaging in Theranostics

Property	¹²⁴ I	¹³¹ I
Physical half-life (h)	100.22	192.50
Radiation	β ⁺ , ε	β ⁻ , γ
Availability	Limited	Common
Cost	Expensive	Low
Imaging system	PET/CT	SPECT/CT
System sensitivity (cps/Bq)	High	Low
Quantification (attenuation, scatter)	Good	Limited
Image quality	High	Low
Clinical spatial resolution (mm)	6–8	14–17
Late imaging (≥96 h)	Yes	Yes
“Stunning effect”	? (No)	High

Most patients typically undergo several radioiodine treatments during their disease history, and each additional radioiodine treatment increases the risk of radiation-associated detrimental effects. To reduce or at least estimate the risks, as well as to increase the efficacy of radioiodine treatment, an individual assessment of absorbed radiation doses to the tumors and the organs at risk is crucial. According to Maxon et al., an absorbed dose of 85 Gy or higher is associated with an 80%–90% likelihood of a therapy response in lymph node metastases (Table 2) (11). The absorbed dose thresholds for other metastatic tissues (and thyroid remnants), derived from current ¹²⁴I PET dosimetry studies, are also shown in Table 2 (12,13). Of note, a response to radioiodine is already expected for absorbed doses exceeding 20 Gy (11,12). Moreover, the bone marrow is often the dose-limiting organ in the application of high therapy activities.

TABLE 2

Relationship Between Absorbed Dose Thresholds and Associated Complete Response Rates for Metastases and Thyroid Remnants

Lesion	Target dose (Gy)	¹²⁴ I PET*	¹³¹ I WBS†
Lymph node metastases	≥85	75%‡	80%–90%
Pulmonary metastases	≥85	95%	Unknown
Bone metastases	≥85	46%	Unknown
	350–650	70%–80%	Unknown
Thyroid remnants	≥300	91%	80%–90%

*Data are from Jentzen et al. (12,13).

†Data are from Maxon and Smith (26). WBS = whole-body scintigraphy.

‡Lymph node metastases with follow-up times of less than 4 mo are included.

Pretherapy blood dosimetry has been developed to estimate the toxicity of radioiodine with the aim of avoiding possible life-threatening, radiation-induced bone marrow suppression (Fig. 1). In this organ-at-risk dosimetry approach, the maximum tolerable ¹³¹I activity that can be safely administered without producing toxic effects is calculated. Through collection of blood samples and determination of external whole-body counts over a period of 4 d or longer, the maximum tolerable ¹³¹I activity can be estimated using an absorbed dose limit of 2 Gy to blood (as a surrogate for bone marrow toxicity) (14–16). The key quantities for estimating the absorbed dose to the tumor are mass (or volume), the initial uptake value (for instance, at 24 h), and the effective ¹³¹I half-life. The mass can be estimated from CT or ¹²⁴I PET using sophisticated threshold-based segmentation algorithms. Determination of the 24-h uptake—mainly mediated through the NIS—and the predicted effective ¹³¹I half-life requires serial ¹²⁴I PET/CT scans (17). Pretherapy dosimetry results enable the selection of an optimized therapeutic activity—that is, the activity achieving a high tumor dose (such as 85 Gy for lymph node metastases) while maintaining a dose less than the 2-Gy limit to blood (Fig. 1). Thus, ¹²⁴I dosimetry is suitable for individual therapy assessment.

IODINE METABOLISM

A better understanding of ¹²⁴I PET dosimetry can be gained through an examination of iodine metabolism (Fig. 2). In brief, iodide is transported actively into the cell

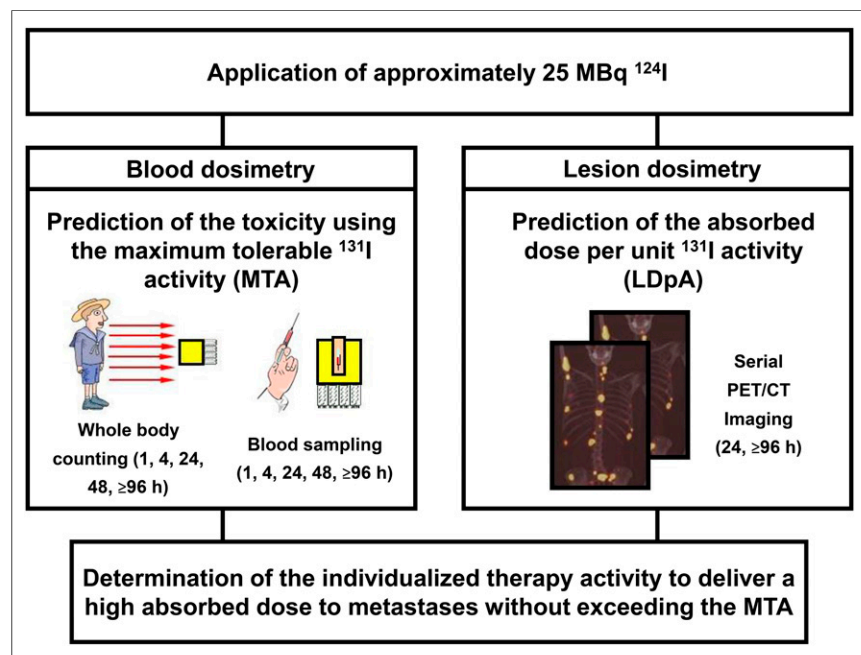


FIGURE 1. Simplified illustration of 2 main pillars of ¹²⁴I dosimetry concept. LDpA = lesion-absorbed dose per administered activity; MTA = maximum tolerable activity.

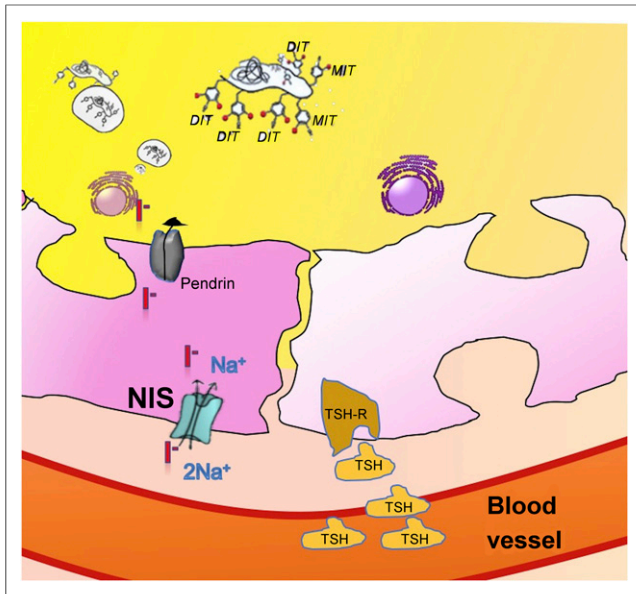


FIGURE 2. Thyroid follicle showing iodine uptake and residence. Expression of NIS is essential for iodide uptake. Iodide is transported via pendrin to colloid in which iodide is bound to thyroglobulin. The latter is crucial to increasing average time on site of radioiodine in the follicle, which is associated with an increased absorbed radiation dose. Non-thyroidal cells expressing NIS lack this storing mechanism. DIT = diiodotyrosine; MIT = monoiodotyrosine; TSH = thyroid-stimulating hormone; TSH-R = TSH receptor. The function of TSH is to stimulate NIS expression.

via the NIS, which is located in the basolateral membrane of thyrocytes. Next, this iodide enters the colloid on the apical membrane, located on the opposite side, via pendrin or other

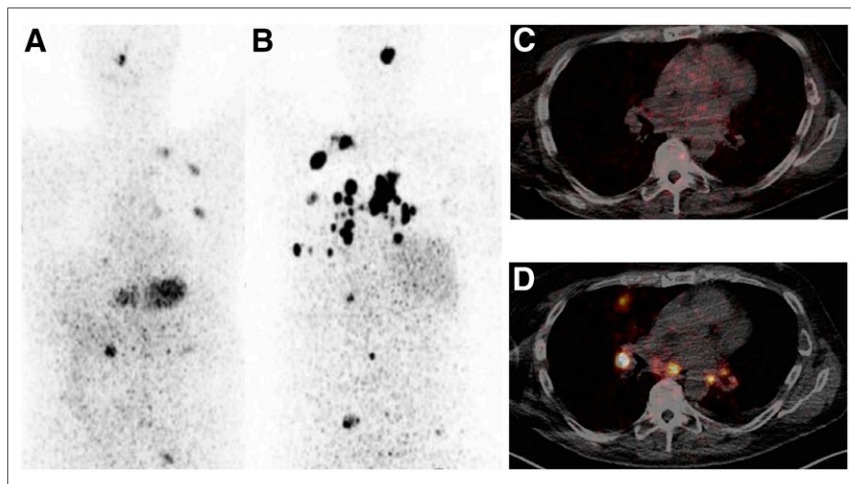


FIGURE 3. PET/CT images of 69-y-old patient with follicular thyroid carcinoma diagnosed in 1999. Patient underwent surgery and many treatments with radioiodine and experienced disease progression involving bone and lymph node metastases. Patient had undergone tyrosine kinase inhibitor treatment with sorafenib and lenvatinib but discontinued treatment because of disease progression. Patient was introduced to our hospital for redifferentiation therapy. After confirmation of BRAF-WT mutation status using archival tumor tissue, patient underwent pretreatment lesion dosimetry under thyrotropin stimulation with recombinant human thyrotropin (A and C). Target lesions showed absorbed doses of 1–10 Gy/GBq. After 4 wk of trametinib treatment, ^{124}I PET lesion dosimetry revealed absorbed doses of 10–322 Gy/GBq for most metastases (B and D). Blood dosimetry estimated maximum tolerable activity of 7 GBq. Patient was treated with 6 GBq of ^{131}I . This example demonstrates importance of in vivo dosimetry in estimating redifferentiation effects and evaluating radioiodine treatment of nonthyroidal tumors.

unspecified channels (18). In the colloid, iodide is oxidized, is bound to thyroglobulin (via the enzyme thyroid peroxidase), and either remains in the colloid or exits the cell as the end product—the thyroid hormone triiodothyronine or tetraiodothyronine. The active transport of iodide into the cell via the NIS is correlated with the level of expression of this symporter and can be estimated in vivo through ^{124}I PET imaging. The effective half-life—that is, the decrease in accumulated radioiodine uptake over time—cannot be quantified on the basis of a single PET scan. Therefore, serial PET scans over time are needed to estimate the kinetics of radioiodine. Even though the precision of the quantification of radioiodine accumulation over time increases with the number of PET scans, these scans are limited in clinical settings for time and economic reasons. Therefore, a 2-time-point model that reasonably balances precision and effort or cost in clinical settings has been developed (19).

An example is provided in Figure 3, which shows ^{124}I PET/CT images of a thyroid cancer patient and describes the lesions along with their predicted absorbed doses. ^{124}I PET was capable of quantifying the increase in NIS expression in this patient with radioiodine-refractory thyroid cancer after redifferentiation treatment with trametinib, a mitogen-activated extracellular signal-related kinase kinase inhibitor. This is the first report of trametinib treatment of a patient with radioiodine-refractory thyroid cancer. Basically, as shown by the ^{124}I PET results, the effective half-lives of the lesions remained similar (Fig. 4). Because of previous experience with mitogen-activated extracellular signal-related kinase inhibition in this setting, we expected an increase in NIS expression without a significant increase in the effective half-lives, as shown in Figure 4 (17). The effects in our patient with radioiodine-refractory thyroid cancer were in line with this expectation. The ^{124}I PET results revealed a 10-fold increase in iodide uptake with a nonsignificant change in the effective half-life.

These findings were most likely due to the fact that in such tumors, mitogen-activated extracellular signal-related kinase inhibition alone is not sufficient to reestablish the polarity of the cells and, thus, reshape a functioning colloidal structure. The latter is crucial for proper binding of iodide to thyroglobulin, resulting in an increased effective half-life. Nevertheless, the increased level of NIS expression alone was sufficient to increase the estimated absorbed dose significantly. The dosimetry results showed that the patient should have been treated with 17 GBq of ^{131}I . However, the decision about a treatment must also be based on the blood dosimetry results, which limited the amount of treatment activity to 7 GBq of ^{131}I . Even though there is no single clinical study analyzing the predictive value of pretherapeutic ^{124}I PET dosimetry, the common consensus is that ^{124}I PET dosimetry contributes significantly to pretherapeutic absorbed dose estimations. The example provided here not only illustrates the potential of ^{124}I PET dosimetry but also underlines the importance of applying this

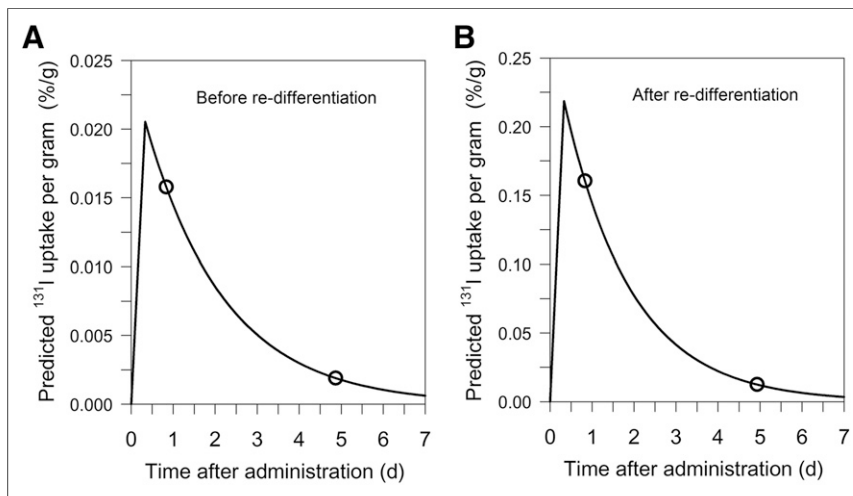


FIGURE 4. Predicted ^{131}I uptake curve derived from ^{124}I PET-based lesion dosimetry before (A) and after (B) redifferentiation. Lines were calculated using 2-point approach (19), and symbols represent measured PET-derived uptake values. Uptake values before differentiation were lower by factor of 10, demonstrating similar effective half-lives but 10-fold-lower 24-h uptake per gram.

dosimetry approach to redifferentiation treatments in clinical routines (20).

THERANOSTICS WITH IODINE IN NONTHYROIDAL CANCER

The simplicity and efficacy of radioiodine for the imaging and treatment of thyroid cancer patients attracted many research groups to investigate NIS expression in nonthyroidal tumor entities with the aim of treating these entities with radioiodine as well (21,22). In this context, some research groups investigated the efficacy of transfection of the NIS gene to tumor cells to make them targets for radioiodine. Table 3 shows the results of a study in which NIS expression in nonthyroidal tumors was investigated. Investigating radioiodine accumulation in nonthyroidal tissue requires an appreciation of the lack of a colloidal structure in the tumor cells and, thus, the absence of an ability to metabolize iodine and the consequent negative impact on the effective half-life of iodine. Given these circumstances, the level of expression

TABLE 3
Extrathyroidal Tissues Expressing NIS

Primary cancer	No. of specimens	NIS expression (%)
Bladder	24	42
Colon	75	63
Lung	58	66
Pancreas	11	64
Prostate	34	74
Ovary	37	73
Testis	107	64
Stomach	27	59
Cervix	11	100

Data are from Wapnir et al. (21).

of the NIS in nonthyroidal tumor cells should compensate for these shortcomings to achieve a significant absorbed dose. This goal is challenging and is probably the main reason why no clinical data showing the efficacy of radioiodine in nonthyroidal tumors have yet been published.

Another issue is the presence of thyroid in patients with nonthyroidal cancer. Because these patients have a functioning thyroid, the applied radioiodine will be actively transported into thyroid cells; therefore, the amount of radioiodine delivered to the targeted tumor cells will be reduced. More important than this reduced efficacy is unintended radiation damage to thyroid cells. However, thyroid uptake can be reduced through the coapplication of triiodothyronine (or tetraiodothyronine) and methimazole. Triiodothyronine downregulates the thyrotropin level (through a feedback loop), resulting in a reduction in NIS expression and, consecutively, a reduction in iodine uptake. Methimazole inhibits the enzyme

thyroperoxidase, which catalyzes the binding of iodine to thyroglobulin and, thus, reduces the effective half-life of iodine (23).

IODINE AND BREAST CANCER

Breast cancer was one of the first nonthyroidal tumor entities in which NIS expression was convincingly shown (by messenger RNA levels and immunohistochemical staining). Therefore, many groups proposed radioiodine treatment for patients with breast cancer expressing the NIS (24,25). However, the *in vivo* imaging of NIS expression (^{131}I or $^{99\text{m}}\text{Tc}$ scans) in the tumor cells did not correlate with NIS expression shown by messenger RNA levels and immunohistochemical staining. This apparently contradictory result is more likely to be due to the fact that the increased expression of the NIS on messenger RNA and protein levels is not translated into a functioning NIS located on the basolateral membrane. The latter is crucial for proper functioning of this symporter.

There are few reports on the imaging of increased NIS expression in breast cancer xenografts and in brain metastases of breast cancer in mice. Kelkar et al. discussed a potential treatment for patients (25). However, no data analyzing this hypothesis in clinical settings have yet been published. The main shortcoming of the published *in vivo* data is that the role of tumor dosimetry—that is, an estimation of the absorbed doses delivered to tumors—was not analyzed. As described earlier, quantifying the uptake, effective half-life, and tumor mass is crucial for calculating the doses delivered to tumors; these data, in turn, predict the response to radioiodine.

Figure 5 shows an estimation of the model-based absorbed doses for a spheric tumor as a function of 24-h ^{131}I uptake per gram and at various effective half-lives. As shown in Figure 4, the 24-h ^{131}I uptake per gram was approximately 0.16%/g after redifferentiation, and the effective half-life was estimated to be 1 d. As shown in Figure 5, the estimated absorbed dose was about 10 Gy/GBq, a value that was similar to the calculated one. This approach may suggest the extent to which the iodide uptake must be increased to achieve a tumoricidal absorbed dose.

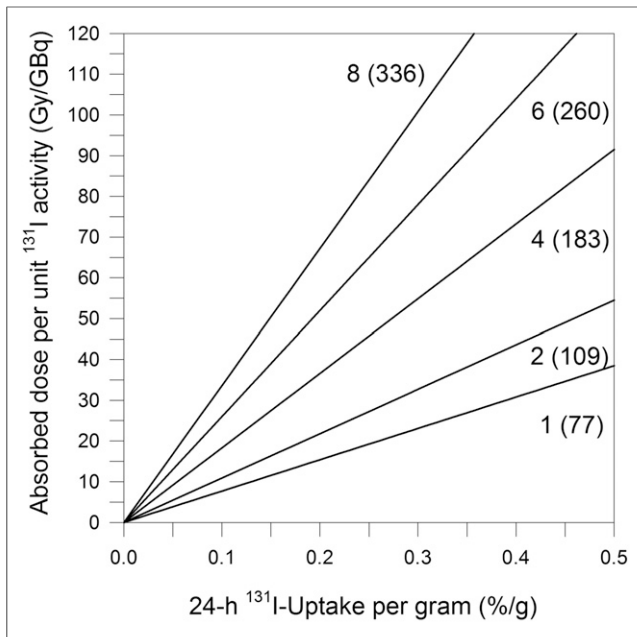


FIGURE 5. Model-based relationship between absorbed dose and actual 24-h ^{131}I uptake per gram of tissue for 1-mL spheric lesion at different effective half-lives (in days) (shown close to straight lines); values within parentheses are estimated slopes (in Gy/GBq per unit percentage uptake per gram) for assessing absorbed doses beyond axis scale limit. Uptake curves decreased monoexponentially using the respective effective half-lives. For volumes ranging from 0.1 to 5 mL, absolute percentage absorbed dose deviations from 1-mL volume were less than or equal to 5%. Nonlinear relationship between slope and half-life resulted from extrapolation from 24-h uptake value to zero time point.

CONCLUSION

Theranostics with the matched pair $^{124}\text{I}/^{131}\text{I}$ in high-risk or progressive thyroid cancer enables an individualized dosimetry approach to delivering high absorbed doses to tumors and reducing radiation-related toxicity primarily to bone marrow. The target dose delivered through ^{131}I depends on iodine uptake and effective half-life. In this context, NIS expression is critical for iodine uptake and a colloidal configuration with polarized thyrocytes for the effective half-life of radioiodine. Therefore, applying radioiodine isotopes to nonthyroidal tumor cells remains challenging, but individualized dosimetry at least facilitates proper analysis of the expected effectiveness.

DISCLOSURE

No potential conflict of interest relevant to this article was reported.

REFERENCES

- Del Vecchio S, Zannetti A, Fonti R, Pace L, Salvatore M. Nuclear imaging in cancer theranostics. *Q J Nucl Med Mol Imaging*. 2007;51:152–163.
- Strosberg J, El-Haddad G, Wolin E, et al. Phase 3 trial of ^{177}Lu -dotatate for midgut neuroendocrine tumors. *N Engl J Med*. 2017;376:125–135.
- Grubmüller B, Baum RP, Capasso E, et al. ^{64}Cu -PSMA-617 PET/CT imaging of prostate adenocarcinoma: first in-human studies. *Cancer Biother Radiopharm*. 2016;31:277–286.

- Kratochwil C, Afshar-Oromieh A, Kopka K, Haberkorn U, Giesel FL. Current status of prostate-specific membrane antigen targeting in nuclear medicine: clinical translation of chelator containing prostate-specific membrane antigen ligands into diagnostics and therapy for prostate cancer. *Semin Nucl Med*. 2016;46:405–418.
- Poeppel TD, Binse I, Petersenn S, et al. ^{68}Ga -DOTATOC versus ^{68}Ga -DOTATATE PET/CT in functional imaging of neuroendocrine tumors. *J Nucl Med*. 2011;52:1864–1870.
- Bodei L, Cremonesi M, Zoboli S, et al. Receptor-mediated radionuclide therapy with ^{90}Y -DOTATOC in association with amino acid infusion: a phase I study. *Eur J Nucl Med Mol Imaging*. 2003;30:207–216.
- Giesel FL, Hadaschik B, Cardinale J, et al. F-18 labelled PSMA-1007: biodistribution, radiation dosimetry and histopathological validation of tumor lesions in prostate cancer patients. *Eur J Nucl Med Mol Imaging*. 2017;44:678–688.
- Kratochwil C, Bruchertseifer F, Giesel FL, et al. ^{225}Ac -PSMA-617 for PSMA-targeted radiation therapy of metastatic castration-resistant prostate cancer. *J Nucl Med*. 2016;57:1941–1944.
- Freudenberg LS, Jentzen W, Görges R, et al. ^{124}I -PET dosimetry in advanced differentiated thyroid cancer: therapeutic impact. *Nuklearmedizin*. 2007;46:121–128.
- Van Nostrand D, Moreau S, Bandaru VV, et al. ^{124}I positron emission tomography versus ^{131}I planar imaging in the identification of residual thyroid tissue and/or metastasis in patients who have well-differentiated thyroid cancer. *Thyroid*. 2010;20:879–883.
- Maxon HR III, Englaro EE, Thomas SR, et al. Radioiodine-131 therapy for well-differentiated thyroid cancer: a quantitative radiation dosimetric approach—outcome and validation in 85 patients. *J Nucl Med*. 1992;33:1132–1136.
- Jentzen W, Hoppenbrouwers J, van Leeuwen P, et al. Assessment of lesion response in the initial radioiodine treatment of differentiated thyroid cancer using ^{124}I PET imaging. *J Nucl Med*. 2014;55:1759–1765.
- Jentzen W, Verschure F, van Zon A, et al. ^{124}I PET assessment of response of bone metastases to initial radioiodine treatment of differentiated thyroid cancer. *J Nucl Med*. 2016;57:1499–1504.
- Lassmann M, Häscheid H, Chiesa C, et al. EANM Dosimetry Committee series on standard operational procedures for pre-therapeutic dosimetry I: blood and bone marrow dosimetry in differentiated thyroid cancer therapy. *Eur J Nucl Med Mol Imaging*. 2008;35:1405–1412.
- Jentzen W, Bockisch A, Ruhlmann M. Assessment of simplified blood dose protocols for the estimation of the maximum tolerable activity in thyroid cancer patients undergoing radioiodine therapy using ^{124}I . *J Nucl Med*. 2015;56:832–838.
- Benua RS, Cicale NR, Sonenberg M, Rawson RW. The relation of radioiodine dosimetry to results and complications in the treatment of metastatic thyroid cancer. *AJR*. 1962;87:171–182.
- Nagarajah J, Le M, Knauf JA, et al. Sustained ERK inhibition maximizes responses of BrafV600E thyroid cancers to radioiodine. *J Clin Invest*. 2016;126:4119–4124.
- Dohán O, De la Vieja A, Paroder V, et al. The sodium/iodide symporter (NIS): characterization, regulation, and medical significance. *Endocr Rev*. 2003;24:48–77.
- Jentzen W, Freudenberg L, Eising EG, Sonnenschein W, Knust J, Bockisch A. Optimized ^{124}I PET dosimetry protocol for radioiodine therapy of differentiated thyroid cancer. *J Nucl Med*. 2008;49:1017–1023.
- Ho AL, Grewal RK, Leboeuf R, et al. Selumetinib-enhanced radioiodine uptake in advanced thyroid cancer. *N Engl J Med*. 2013;368:623–632.
- Wapnir IL, van de Rijn M, Nowels K, et al. Immunohistochemical profile of the sodium/iodide symporter in thyroid, breast, and other carcinomas using high density tissue microarrays and conventional sections. *J Clin Endocrinol Metab*. 2003;88:1880–1888.
- Micali S, Bulotta S, Puppini C, et al. Sodium iodide symporter (NIS) in extra-thyroidal malignancies: focus on breast and urological cancer. *BMC Cancer*. 2014;14:303.
- Wapnir IL, Goris ML, Yudd AP, et al. The Na/I-symporter mediates iodide uptake in breast cancer metastases and can be selectively down-regulated in the thyroid. *Clin Cancer Res*. 2004;10:4294–4302.
- Renier C, Do J, Reyna-Neyra A, et al. Regression of experimental NIS-expressing breast cancer brain metastases in response to radioiodide/gemcitabine dual therapy. *Oncotarget*. 2016;7:54811–54824.
- Kelkar MG, Senthilkumar K, Jadhav S, Gupta S, Ahn BC, De A. Enhancement of human sodium iodide symporter gene therapy for breast cancer by HDAC inhibitor mediated transcriptional modulation. *Sci Rep*. 2016;6:19341.
- Maxon HR, Smith HS. Radioiodine-131 in the diagnosis and treatment of metastatic well differentiated thyroid cancer. *Endocrinol Metab Clin North Am*. 1990;19:685–718.